Bol. Soc. Paran. Mat.
©SPM – E-ISSN-2175-1188
SPM: www.spm.uem.br/bspm

(3s.) **v. 2025 (43)** : 1–18.
ISSN-0037-8712
doi:10.5269/bspm.77266

Study of Monkeypox Virus Transmission Dynamics: Vaccination Effect and Sensitivity Analysis

Himani Agrawal, Atar Singh, Shyamsunder*, S.D. Purohit, Ali Akgül

ABSTRACT: Monkeypox is an emerging infectious disease from Nigeria that has spread globally, affecting countries such as the USA and the United Kingdom. It belongs to the Poxviridae family under the Orthopoxvirus genus. In this study, we develop a deterministic compartmental model comprising eleven classes: susceptible, vaccinated, exposed, quarantined, hospitalized, and recovered humans, along with susceptible, exposed, infected, and recovered rodents. We analyze the disease-free equilibrium and calculate the basic reproduction number using the next-generation matrix approach. Sensitivity analysis identifies critical parameters influencing disease transmission. Numerical simulations conducted in MATLAB demonstrate that increasing vaccination coverage among humans significantly reduces infection prevalence. The results further reveal that timely quarantine and hospitalization effectively control the spread of the virus. Our findings provide quantitative evidence supporting vaccination and control interventions as vital strategies to mitigate monkeypox outbreaks.

Key Words: Monkeypox virus, mathematical model, reproduction number, sensitivity analysis.

Contents

1. Introduction

Over along with the few century, Novel illnesses have arisen in diverse places worldwide. Monkeypox (Mpox) disease is also one of them. Mpox is a viral disease caused by the MPXV [1], classified under the orthopox virus genus in the Poxviriade family. Three more human viruses belong to this category: the vaccinia virus, the variola virus, and the cowpox virus, which causes smallpox [2, 3]. Mpox and smallpox share similar clinical symptoms. The condition has developed as a severe public health concern throughout Africa, particularly in the central and western regions, because it primarily affects individuals who live near tropical rainforests. Researchers have increasingly focused on viruses over the past couple of years, seeking treatment for these ailments [4]. The first human case of the zoonotic ortho-pox DNA virus is Mpox. It occurred in the democratic republic of the Congo in 1970 [5], which had previously

* Corresponding author.
2010 *Mathematics Subject Classification:* 92B05, 92D30, 00A71.
Submitted June 09, 2025. Published September 17, 2025

been seen as smallpox. Since that time, the majority of cases have been recorded in rural regions of central and western Africa. This virus has spread to the Congo, Benin, Cameroon, Gabon, Nigeria, and elsewhere.

Nigeria saw one of the crucify eruption in 2017 [6, 7], with 200 confirmed cases, 500 suspected cases, and a 3% death rate, and cases are still being recorded up to this day. A further outbreak outside of Africa happened in the USA in 2007 and was directly related to an infected pet, nominated as patient zero [8]. There were 70 confirmed cases as a result of this outbreak. With the continued identification of confirmed cases, more research is needed to appreciate the immunology, transmission patterns, and source of Mpox infection and develop treatments and vaccines. Mpox, a recently resurfaced virus since June 2022, has garnered significant interest among researchers striving to develop novel preventive measures to manage such viruses.

Between the crucial period (May 13 to May 21, 2022), a total of 92 obsessive cases were stated in many non-endemic regions, with no deaths reported so far. Mpox is a zoonotic viral disease. It mainly affects animals, especially monkeys, squirrels, and rodents. This illness can roll out from animals to people [9–11]. It can also roll out from person to person by close contact with infected people, typically through the transmission of gasping droplets or direct contact with skin pores and bodily fluids [12–14]. In addition to these mechanisms, it can be transferred by contact with contaminated surfaces or objects, referred to as ecological dissemination [15, 16].

The organization of this paper is as follows: In Section (2), we develop our model with the explanation. Section (3) provides the bounded solution with positivity. Section (4) describes equilibria analysis in which we have found some equilibrium points and basic reproduction numbers. Section (5) represents the stability analysis of the model. In Section (6), we investigate the sensitivity of the model. Section (7) describes numerical simulation with a graphical discussion of this proposed model. The last Section (8) concludes with the results and discussion of this paper.

2. Model formulation

This section seeks to construct a compartmental system to examine the the kinetics of MPXV spread in humans and primates who are not human (wild animals) [17]. We have categorized the two kinds whereas, the human populace is classified into seven compartments, namely susceptible human populace $S_h(t)$, vaccinated human populace $V_h(t)$, exposed human populace $E_h(t)$, quarantined human populace $Q_h(t)$, infectious human populace $I_h(t)$, recovered (removed) human populace $R_h(t)$, hospitalized human populace $H_h(t)$ and the rodent populace are classified as susceptible rodent populace $S_r(t)$, exposed rodent populace $E_r(t)$, infectious rodent populace $I_r(t)$, and recovered (removed) rodent populace $R_r(t)$.

Birth and demise represent the two fundamental processes through which individuals are connected to humanity, occurring at rates of Λ_h and μ_h, respectively. The rodent populace's birth and death rates are shown as Λ_r and μ_r, respectively. Upon contact with an individual infected with MPXV, a healthy person may become infected. Upon the manifestation of symptoms associated with the illness within a time frame of 10 to 25 days, individuals are classified as part of the infected compartment. The parameter α_h represents the transmission rate of the vaccine. In the event that the virus remains uncured, individuals in the vaccinated populace transition to the exposed populace at a rate of γI_h. The susceptible populace transitions into the exposed class at rates of β_1 and β_2. The exposed populace is categorized into three distinct compartments: I_h, Q_h, and H_h. Each compartment is associated with rates of α_1, α_2, and α_3, respectively. Nonetheless, the quarantined human populace transitioned back to the susceptible compartment at a rate of ξ. At the rate of τ_1, the quarantined human populace is admitted to a hospital, while at the rate of τ_2, the quarantined populace experiences direct recovery. The admission rate of the infected human populace to the hospital is denoted as ζ. The infected populace exhibited a recovery rate of ρ_h, while the hospitalized populace demonstrated a recovery rate of β. d_h presents the rate of disease spread among quarantined, hospitalized, and infected individuals. Rodents that are susceptible are exposed at a rate of $\delta_r I_r$. Exposed rodents transform infected α_4 is a rate of transform, and infected rodents recover at a rate of ρ_r. The parameter d_r represents the transmission rate of infectious diseases among rodent populaces. It is believed that individuals who have been vaccinated will not contract the disease at any point in their lives. In contrast, individuals who have not been successfully vaccinated are exposed at a rate denoted as γ. This group of humans is similarly affected,

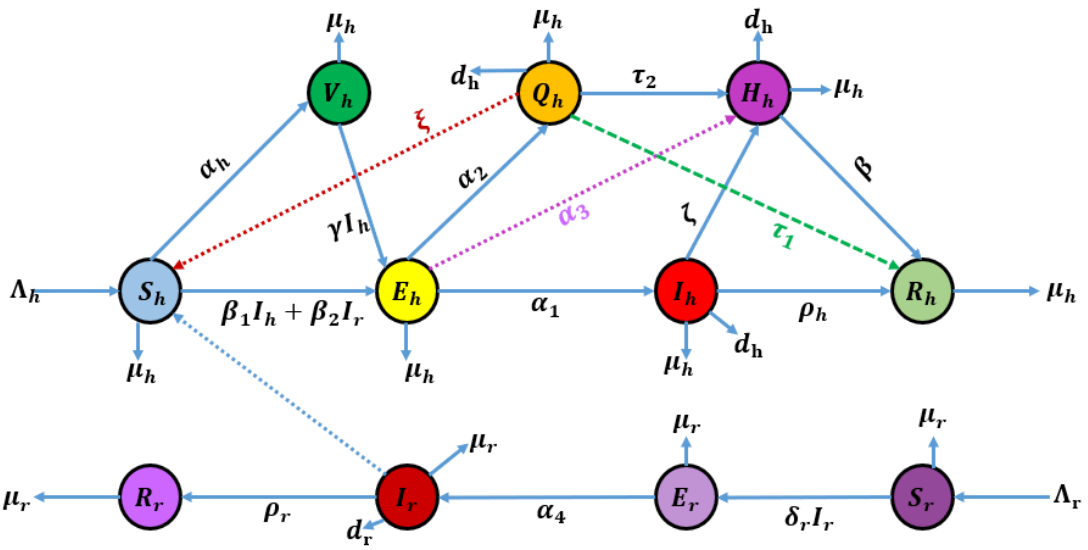

Figure 1: Schematic flow diagram of $S_hV_hE_hQ_hI_hH_hR_hS_rE_rI_rR_r$.

and it is also believed that transmission to rodents does not occur through human contact. Figure 1 illustrates the parameters transmitted from each compartment and the interactions occurring between the human and rodent populaces.

$$
\begin{aligned}
\frac{dS_h}{dt} &= \Lambda_h - (\alpha_h + \mu_h)S_h(t) + \xi Q_h(t) - (\beta_1 I_h(t) + \beta_2 I_r(t))S_h(t),\\
\frac{dV_h}{dt} &= \alpha_h S_h(t) - \mu_h V_h(t) - \gamma V_h(t) I_h(t),\\
\frac{dE_h}{dt} &= \gamma V_h(t) I_h(t) + (\beta_1 I_h(t) + \beta_2 I_r(t))S_h(t) - (\alpha_2 + \mu_h + \alpha_3 + \alpha_1)E_h(t),\\
\frac{dQ_h}{dt} &= \alpha_2 E_h(t) - (\xi + \mu_h + \tau_1 + d_h + \tau_2)Q_h(t),\\
\frac{dI_h}{dt} &= \alpha_1 E_h(t) - (\zeta + \mu_h + \rho_h + d_h)I_h(t),\\
\frac{dH_h}{dt} &= \zeta I_h(t) + \alpha_3 E_h(t) + \tau_2 Q_h(t) - (\beta + \mu_h + d_h)H_h(t),\\
\frac{dR_h}{dt} &= \rho_h I_h(t) + \tau_1 Q_h(t) + \beta H_h(t) - \mu_h R_h(t),\\
\frac{dS_r}{dt} &= \Lambda_r - \mu_r S_r(t) - \delta_r S_r(t) I_r(t),\\
\frac{dE_r}{dt} &= \delta_r S_r(t) I_r(t) - (\mu_r + \alpha_4)E_r(t),\\
\frac{dI_r}{dt} &= \alpha_4 E_r(t) - (\rho_r + \mu_r + d_r)I_r(t),\\
\frac{dR_r}{dt} &= \rho_r I_r(t) - \mu_r R_r(t),
\end{aligned}
\tag{2.1}
$$

with starting conditions $S_h(0) = S_{h0}$, $V_h(0) = V_{h0}$, $E_h(0) = E_{h0}$, $Q_h(0) = Q_{h0}$, $I_h(0) = I_{h0}$, $H_h(0) = H_{h0}$, $R_h(0) = R_{h0}$, $S_r(0) = S_{r0}$, $E_r(0) = E_{r0}$, $I_r(0) = I_{r0}$, $R_r(0) = R_{r0}$.

3. Qualitative assessment of the model

This section, we discuss the topics of boundedness and positivity of solutions in more detail through essential theorems.

3.1. Boundedness

The developed Mpox model (2.1) viable area is $\Omega = \Omega_h \times \Omega_r$ is the proper set of $\mathbb{R}^7_+ \times \mathbb{R}^4_+$, where,
$\Omega_h = \{(S_h(t), V_h(t), E_h(t), Q_h(t), I_h(t), H_h(t), R_h(t) \subseteq \mathbb{R}^7_+ : 0 < N_h \leq \frac{\Lambda_h}{\mu_h}\}$ and $\Omega_r = \{(S_r, E_r, I_r, R_r) \subseteq \mathbb{R}^4_+ : 0 < N_r \leq \frac{\Lambda_r}{\mu_r}\}$.

Theorem 3.1 *The area indicated by $\Omega = \Omega_h \times \Omega_r$ is a positively stable collection for model (2.1).*

Proof 3.1 *The whole human population $N_h = S_h + V_h + E_h + Q_h + I_h + H_h + R_h$. Thus,*

$$\frac{dN_h}{dt} = \frac{dS_h}{dt} + \frac{dV_h}{dt} + \frac{dE_h}{dt} + \frac{dQ_h}{dt} + \frac{dI_h}{dt} + \frac{dH_h}{dt} + \frac{dR_h}{dt},$$
$$\frac{dN_h}{dt} \leq \Lambda_h - \mu_h \times N_h,$$
$$\lim_{t \longrightarrow \infty} N_h(t) \leq \frac{\Lambda_h}{\mu_h}.$$

As a result, for all positive time values, $N_h(t)$ converges as t approaches infinity. Consequently, the model's solution (2.1) with a starting condition in Ω stays in Ω. Incorporating the final four model (2.1) equations together, we now get

$$\frac{dN_r}{dt} = \frac{dS_r}{dt} + \frac{dE_r}{dt} + \frac{dI_r}{dt} + \frac{dR_r}{dt},$$
$$\frac{dN_r}{dt} = \Lambda_r - \mu_r \times N_r,$$
$$\frac{dN_r}{dt} + \mu_r \times N_r \leq \Lambda_r.$$

Thus, $\lim_{t \longrightarrow \infty} N_r(t) \leq \frac{\Lambda_r}{\mu_r}$. Likewise, for all non-negative values of time, $N_r(t)$ converges for t approaches to infinity; thus, the model's solution (2.1) with starting condition in Ω stays in Ω. This results in the deduction that, in $\Omega = \Omega_h \times \Omega_r$, the region is well-posed and epidemiologically viable.

3.2. Positiveness of Solution

Theorem 3.2 *For any $t \in [0, \infty)$, all solutions of the model (2.1) are non-negative, given that the beginning conditions meet $S_h(0) \geq 0, V_h(0) \geq 0, E_h(0) \geq 0, I_h(0) \geq 0, Q_h(0) \geq 0, H_h(0) \geq 0, R_h(0) \geq 0, S_r(0) \geq 0, E_r(0) \geq 0, I_r(0) \geq 0, R_r(0) \geq 0$.*

Proof 3.2 *Let $W = \sup\{t \geq 0 : S_h(t) \geq 0,\ V_h(t) \geq 0,\ E_h(t) \geq 0,\ I_h(t) \geq 0,\ Q_h(t) \geq 0,\ H_h(t) \geq 0,\ R_h(t) \geq 0,\ S_r(t) \geq 0,\ E_r(t) \geq 0,\ I_r(t) \geq 0,\ R_r(t) \geq 0\}$ there exist t is the element of $[0, \infty)$. Obviously $W > 0$ and $W < \infty$ from system (2.1).*

$$\frac{dS_h}{dt} + (\mu_h + \alpha_h + \beta_1 I_h + \beta_2 I_r) S_h(t) \geq \Lambda_h, \tag{3.1}$$

let $\mu_h + \alpha_h + \beta_1 I_h + \beta_2 I_r = \lambda_1$,

$$\frac{dS_h}{dt} + \lambda_1 S_h(t) \geq \Lambda_h.$$

By applying the method of integrating factors, we have that

$$\frac{d}{dt}\Big(S_h \exp\Big(\int_0^t \lambda_1(t)dt\Big)\Big) \geq \Lambda_h \exp\Big(\int_0^t \lambda_1(t)dt\Big).$$

The following results will occur when you take an integral

$$S_h \geq \left(S_h(0) + \int_0^t \Lambda_h \exp\Big(\int_0^\tau \lambda_1(\tau)d\tau\Big)dt\right)\exp\Big(\int_0^t -\lambda_1(t)dt\Big) \geq 0.$$

Using the same method, it is easily demonstrated that, $V_h(t) \geq 0$, $E_h(t) \geq 0$, $I_h(t) \geq 0$, $Q_h(t) \geq 0$, $H_h(t) \geq 0$, $R_h(t) \geq 0$, $S_r(t) \geq 0$, $E_r(t) \geq 0$, $I_r(t) \geq 0$, $R_r(t) \geq 0$. *For any* $t \in [0, \infty)$, *any model's solution* (2.1) *is non-negative. The aforementioned integration demonstrates positive results in epidemiology.*

Theorem 3.3 *Let us consider* $f : \mathbb{L} \subseteq \mathbb{R} \times \mathbb{R}^n \to \mathbb{R}$ *be a continuous function for every point in the area* $\vartheta|t - t_0| \leq a, ||z - z_0|| \leq b$, *where* $z = (z_1, z_2, z_3, \cdots, z_n)$ *and* $z_0 = (z_{10}, z_{20}, z_{30}, \cdots, z_{n0})$, $\|f(t, z)\| \leq M$ *and* $f(x, z)$ *satisfies Lipschitz condition,* $||f(t, \bar{z_1}) - f(t, \bar{z_2})|| \leq \bar{K}||\bar{t_1} - \bar{t_2}||, \bar{K} > 0$ *then for any pairs* $(t, \bar{z_1}), (t, \bar{z_2}) \in \vartheta\ \exists\ \delta > 0$ *such that there is a unique solution* $z(t)$ *of the system* $\frac{dz}{dt} = f(t, z) \in |t - t_0| < \delta$.

Theorem 3.4 *If* $\frac{\partial f}{\partial z_j}$ *is continuous on a closed, convex , and bounded domain in* $\mathbb{R}$, *then* f *is Lipschitz.*

Theorem 3.5 *Suppose that* $\mathbb{L} \subseteq \mathbb{R} \times \mathbb{R}^n$ *be the domain described in Theorem 3.3. According to Theorem 3.4, a unique solution exists in the system* (2.1).

Proof 3.3 *Let*

$$\begin{aligned}
M_1 &= \Lambda_h + \xi Q_h(t) - (\mu_h + \alpha_h)S_h(t) - (\beta_1 I_h(t) + \beta_2 I_r(t))S_h(t),\\
M_2 &= \alpha_h S_h(t) - \mu_h V_h(t) - \gamma V_h(t) I_h(t),\\
M_3 &= (\beta_1 I_h(t) + \beta_2 I_r(t))S_h(t) - (\alpha_1 + \mu_h + \alpha_2 + \alpha_3)E_h(t) + \gamma V_h(t) I_h(t),\\
M_4 &= \alpha_2 E_h(t) - (\xi + \mu_h + d_h + \tau_1 + \tau_2)Q_h(t),\\
M_5 &= \alpha_1 E_h(t) - (\mu_h + \rho_h + \zeta + d_h)I_h(t),\\
M_6 &= \zeta I_h(t) + \alpha_3 E_h(t) + \tau_2 Q_h(t) - (\beta + \mu_h + d_h)H_h(t),\\
M_7 &= \rho_h I_h(t) + \tau_1 Q_h(t) + \beta H_h(t) - \mu_h R_h(t),\\
M_8 &= \Lambda_r - \mu_r S_r(t) - \delta_r S_r(t) I_r(t),\\
M_9 &= \delta_r S_r(t) I_r(t) - (\alpha_4 + \mu_r)E_r(t),\\
M_{10} &= \alpha_4 E_r(t) - (d_r + \rho_r + \mu_r)I_r(t),\\
M_{11} &= \rho_r I_r(t) - \mu_r R_r(t).
\end{aligned}$$

We demonstrate the boundedness and continuity of $\frac{\partial M_i}{\partial z_j}, i, j = 1, 2, 3, \cdots, n$. *We have looked at each model equation's partial derivatives* (2.1)*:*

$$\begin{aligned}
&\left|\frac{\partial M_1}{\partial S_h}\right| = |-(\mu_h + \alpha_h) - (\beta_1 I_h + \beta_2 I_r)| < \infty, \left|\frac{\partial M_1}{\partial V_h}\right| = |0| < \infty, \quad \left|\frac{\partial M_1}{\partial E_h}\right| = |0| < \infty,\\
&\left|\frac{\partial M_1}{\partial Q_h}\right| = |\xi| < \infty, \left|\frac{\partial M_1}{\partial I_h}\right| = |-\beta_1 S_h| < \infty, \left|\frac{\partial M_1}{\partial H_h}\right| = |0| < \infty, \quad \left|\frac{\partial M_1}{\partial R_h}\right| = |0| < \infty,\\
&\left|\frac{\partial M_1}{\partial S_r}\right| = |0| < \infty, \left|\frac{\partial M_1}{\partial E_r}\right| = |0| < \infty, \quad \left|\frac{\partial M_1}{\partial I_r}\right| = |-\beta_2 S_h| < \infty, \left|\frac{\partial M_1}{\partial R_r}\right| = |0| < \infty.
\end{aligned}$$

Similarly for M_2

$$\begin{aligned}
&\left|\frac{\partial M_2}{\partial S_h}\right| = |\alpha_h| < \infty, \quad \left|\frac{\partial M_2}{\partial V_h}\right| = |-\mu_h - \gamma I_h| < \infty, \left|\frac{\partial M_2}{\partial E_h}\right| = |0| < \infty, \quad \left|\frac{\partial M_2}{\partial Q_h}\right| = |0| < \infty,\\
&\left|\frac{\partial M_2}{\partial I_h}\right| = |-\gamma V_h| < \infty, \left|\frac{\partial M_2}{\partial H_h}\right| = |0| < \infty, \quad \left|\frac{\partial M_2}{\partial R_h}\right| = |0| < \infty, \quad \left|\frac{\partial M_2}{\partial S_r}\right| = |0| < \infty,\\
&\left|\frac{\partial M_2}{\partial E_r}\right| = |0| < \infty, \quad \left|\frac{\partial M_2}{\partial I_r}\right| = |0| < \infty, \quad \left|\frac{\partial M_2}{\partial R_r}\right| = |0| < \infty.
\end{aligned}$$

Similarly for M_3

$$\left|\frac{\partial M_3}{\partial S_h}\right| = |\beta_1 I_h + \beta_2 I_h| < \infty, \quad \left|\frac{\partial M_3}{\partial V_h}\right| = |\gamma I_h| < \infty, \quad \left|\frac{\partial M_3}{\partial E_h}\right| = |-(\alpha_1+\alpha_2+\alpha_3+\mu_h)| < \infty,$$
$$\left|\frac{\partial M_3}{\partial Q_h}\right| = |0| < \infty, \quad \left|\frac{\partial M_3}{\partial I_h}\right| = |\beta_1 S_h + \gamma V_h| < \infty, \quad \left|\frac{\partial M_3}{\partial H_h}\right| = |0| < \infty, \quad \left|\frac{\partial M_3}{\partial R_h}\right| = |0| < \infty,$$
$$\left|\frac{\partial M_3}{\partial S_r}\right| = |0| < \infty, \quad \left|\frac{\partial M_3}{\partial E_r}\right| = |0| < \infty, \quad \left|\frac{\partial M_3}{\partial I_r}\right| = |\beta_2 S_h| < \infty, \left|\frac{\partial M_3}{\partial R_r}\right| = |0| < \infty.$$

Similarly for M_4

$$\left|\frac{\partial M_4}{\partial S_h}\right| = |0| < \infty, \quad \left|\frac{\partial M_4}{\partial V_h}\right| = |0| < \infty, \quad \left|\frac{\partial M_4}{\partial E_h}\right| = |\alpha_2| < \infty, \quad \left|\frac{\partial M_4}{\partial Q_h}\right| = |-(\tau_1+\tau_2+d_h+\xi+\mu_h)| < \infty,$$
$$\left|\frac{\partial M_4}{\partial I_h}\right| = |0| < \infty, \quad \left|\frac{\partial M_4}{\partial H_h}\right| = |0| < \infty, \quad \left|\frac{\partial M_4}{\partial R_h}\right| = |0| < \infty, \quad \left|\frac{\partial M_4}{\partial S_r}\right| = |0| < \infty,$$
$$\left|\frac{\partial M_4}{\partial E_r}\right| = |0| < \infty, \quad \left|\frac{\partial M_4}{\partial I_r}\right| = |0| < \infty, \quad \left|\frac{\partial M_4}{\partial R_r}\right| = |0| < \infty.$$

Similarly for M_5

$$\left|\frac{\partial M_5}{\partial S_h}\right| = |0| < \infty, \quad \left|\frac{\partial M_5}{\partial V_h}\right| = |0| < \infty, \quad \left|\frac{\partial M_5}{\partial E_h}\right| = |\alpha_1| < \infty, \quad \left|\frac{\partial M_5}{\partial Q_h}\right| = |0| < \infty,$$
$$\left|\frac{\partial M_5}{\partial I_h}\right| = |-(d_h+\mu_h+\zeta+\rho_h)| < \infty, \quad \left|\frac{\partial M_5}{\partial H_h}\right| = |0| < \infty, \quad \left|\frac{\partial M_5}{\partial R_h}\right| = |0| < \infty,$$
$$\left|\frac{\partial M_5}{\partial S_r}\right| = |0| < \infty, \quad \left|\frac{\partial M_5}{\partial E_r}\right| = |0| < \infty, \quad \left|\frac{\partial M_5}{\partial I_r}\right| = |0| < \infty, \quad \left|\frac{\partial M_5}{\partial R_r}\right| = |0| < \infty.$$

Similarly for M_6

$$\left|\frac{\partial M_6}{\partial S_h}\right| = |0| < \infty, \quad \left|\frac{\partial M_6}{\partial V_h}\right| = |0| < \infty, \quad \left|\frac{\partial M_6}{\partial E_h}\right| = |\alpha_3| < \infty, \quad \left|\frac{\partial M_6}{\partial Q_h}\right| = |\tau_2| < \infty,$$
$$\left|\frac{\partial M_6}{\partial I_h}\right| = |\zeta| < \infty, \quad \left|\frac{\partial M_6}{\partial H_h}\right| = |-(\beta+\mu_h+d_h)| < \infty, \quad \left|\frac{\partial M_6}{\partial R_h}\right| = |0| < \infty,$$
$$\left|\frac{\partial M_6}{\partial S_r}\right| = |0| < \infty, \quad \left|\frac{\partial M_6}{\partial E_r}\right| = |0| < \infty, \quad \left|\frac{\partial M_6}{\partial I_r}\right| = |0| < \infty, \quad \left|\frac{\partial M_6}{\partial R_r}\right| = |0| < \infty.$$

Similarly for M_7

$$\left|\frac{\partial M_7}{\partial S_h}\right| = |0| < \infty, \quad \left|\frac{\partial M_7}{\partial V_h}\right| = |0| < \infty, \quad \left|\frac{\partial M_7}{\partial E_h}\right| = |0| < \infty, \quad \left|\frac{\partial M_7}{\partial Q_h}\right| = |\tau_1| < \infty,$$
$$\left|\frac{\partial M_7}{\partial I_h}\right| = |\rho_h| < \infty, \quad \left|\frac{\partial M_7}{\partial H_h}\right| = |\beta| < \infty, \quad \left|\frac{\partial M_7}{\partial R_h}\right| = |-\mu_h| < \infty, \quad \left|\frac{\partial M_7}{\partial S_r}\right| = |0| < \infty,$$
$$\left|\frac{\partial M_7}{\partial E_r}\right| = |0| < \infty, \quad \left|\frac{\partial M_7}{\partial I_r}\right| = |0| < \infty, \quad \left|\frac{\partial M_7}{\partial R_r}\right| = |0| < \infty.$$

Similarly for M_8

$$\left|\frac{\partial M_8}{\partial S_h}\right| = |0| < \infty, \quad \left|\frac{\partial M_8}{\partial V_h}\right| = |0| < \infty, \quad \left|\frac{\partial M_8}{\partial E_h}\right| = |0| < \infty, \quad \left|\frac{\partial M_8}{\partial Q_h}\right| = |0| < \infty,$$
$$\left|\frac{\partial M_8}{\partial I_h}\right| = |0| < \infty, \quad \left|\frac{\partial M_8}{\partial H_h}\right| = |0| < \infty, \quad \left|\frac{\partial M_8}{\partial R_h}\right| = |0| < \infty, \quad \left|\frac{\partial M_8}{\partial S_r}\right| = |-\mu_r-\delta_r I_r| < \infty,$$
$$\left|\frac{\partial M_8}{\partial E_r}\right| = |0| < \infty, \quad \left|\frac{\partial M_8}{\partial I_r}\right| = |-\delta_r S_r| < \infty, \quad \left|\frac{\partial M_8}{\partial R_r}\right| = |0| < \infty.$$

Similarly for M_9

$$\left|\frac{\partial M_9}{\partial S_h}\right| = |0| < \infty, \quad \left|\frac{\partial M_9}{\partial V_h}\right| = |0| < \infty, \quad \left|\frac{\partial M_9}{\partial E_h}\right| = |0| < \infty, \quad \left|\frac{\partial M_9}{\partial Q_h}\right| = |0| < \infty,$$
$$\left|\frac{\partial M_9}{\partial I_h}\right| = |0| < \infty, \quad \left|\frac{\partial M_9}{\partial H_h}\right| = |0| < \infty, \quad \left|\frac{\partial M_9}{\partial R_h}\right| = |0| < \infty, \quad \left|\frac{\partial M_9}{\partial S_r}\right| = |\delta_r I_r| < \infty,$$
$$\left|\frac{\partial M_9}{\partial E_r}\right| = |-(\alpha_4+\mu_r)| < \infty, \quad \left|\frac{\partial M_9}{\partial I_r}\right| = |\delta_r S_r| < \infty, \quad \left|\frac{\partial M_9}{\partial R_r}\right| = |0| < \infty.$$

Similarly for M_{10}

$$\left|\frac{\partial M_{10}}{\partial S_h}\right| = |0| < \infty, \quad \left|\frac{\partial M_{10}}{\partial V_h}\right| = |0| < \infty, \quad \left|\frac{\partial M_{10}}{\partial E_h}\right| = |0| < \infty, \quad \left|\frac{\partial M_{10}}{\partial Q_h}\right| = |0| < \infty,$$
$$\left|\frac{\partial M_{10}}{\partial I_h}\right| = |0| < \infty, \quad \left|\frac{\partial M_{10}}{\partial H_h}\right| = |0| < \infty, \quad \left|\frac{\partial M_{10}}{\partial R_h}\right| = |0| < \infty, \quad \left|\frac{\partial M_{10}}{\partial S_r}\right| = |0| < \infty,$$
$$\left|\frac{\partial M_{10}}{\partial E_r}\right| = |\alpha_4| < \infty, \quad \left|\frac{\partial M_{10}}{\partial I_r}\right| = |-(d_r + \mu_r + \rho_r)| < \infty, \quad \left|\frac{\partial M_{10}}{\partial R_r}\right| = |0| < \infty.$$

Similarly for M_{11}

$$\left|\frac{\partial M_{11}}{\partial S_h}\right| = |0| < \infty, \quad \left|\frac{\partial M_{11}}{\partial V_h}\right| = |0| < \infty, \quad \left|\frac{\partial M_{11}}{\partial E_h}\right| = |0| < \infty, \quad \left|\frac{\partial M_{11}}{\partial Q_h}\right| = |0| < \infty,$$
$$\left|\frac{\partial M_{11}}{\partial I_h}\right| = |0| < \infty, \quad \left|\frac{\partial M_{11}}{\partial H_h}\right| = |0| < \infty, \quad \left|\frac{\partial M_{11}}{\partial R_h}\right| = |0| < \infty, \quad \left|\frac{\partial M_{11}}{\partial S_r}\right| = |0| < \infty,$$
$$\left|\frac{\partial M_{11}}{\partial E_r}\right| = |0| < \infty, \quad \left|\frac{\partial M_{11}}{\partial I_r}\right| = |\rho_r| < \infty, \quad \left|\frac{\partial M_{11}}{\partial R_r}\right| = |-\mu_r| < \infty.$$

We have proved that these partial derivatives are bounded and continuous; hence, in the region $\mathbb{L}$*, there is a unique solution, the system* (2.1)*, as per Theorem 3.5.*

4. Equilibria analysis

This section, we have discussed equilibrium points, reproduction numbers, and stability of reproduction numbers in detail.

4.1. Equilibrium analysis

Equilibrium points for the model (2.1) be equalize all the right hand side will be zero. Then we get Mpox free equilibrium points for both population are free from disease and it is expressed by E^0 described below:

E^0=$(S_h^0, V_h^0, E_h^0, Q_h^0, I_h^0, H_h^0, R_h^0, S_r^0, E_r^0, I_r^0, R_r^0) = \left(\frac{\Lambda_h}{\alpha_h+\mu_h}, \frac{\alpha_h\Lambda_h}{\mu_h(\alpha_h+\mu_h)}, 0, 0, 0, 0, 0, \frac{\Lambda_r}{\mu_r}, 0, 0, 0\right)$.

4.2. Fundamental reproduction number

The fundamental reproduction number for the proposed model can be regulated through the utilization of the next-generation matrix [18]. In the sense, we think about the non-negative matrix $\mathbb{F}$ and the non-singular matrix $\mathbb{V}$ indicating the generation of infection with the transition part in that order, Our $S_hV_hE_hQ_hI_hH_hR_hS_rE_rI_rR_r$ system (2.1) is characterized as follows:

$\frac{dZ}{dt} = F\ (Z) - V\ (Z)$,

where $Z = (E_h, Q_h, I_h, H_h, E_r, I_r)^T$,

$$F = \begin{bmatrix} (\beta_1 I_h + \beta_2 I_r)S_h + \gamma V_h I_h \\ 0 \\ 0 \\ 0 \\ \delta_r S_r I_r \\ 0 \end{bmatrix}$$

$$V = \begin{bmatrix} (\mu_h + \alpha_1 + \alpha_2 + \alpha_3)E_h \\ -\alpha_2 E_h + (\xi + \mu_h + d_h + \tau_1 + \tau_2)Q_h \\ -\alpha_1 E_h + (\mu_h + d_h + \zeta + \rho_h)I_h \\ -\alpha_3 E_h - \zeta I_h - \tau_2 Q_h + (\beta + \mu_h + d_h)H_h \\ (\mu_r + \alpha_4)E_r \\ -\alpha_4 E_r + (\mu_r + d_r + \rho_r)I_r \end{bmatrix}.$$

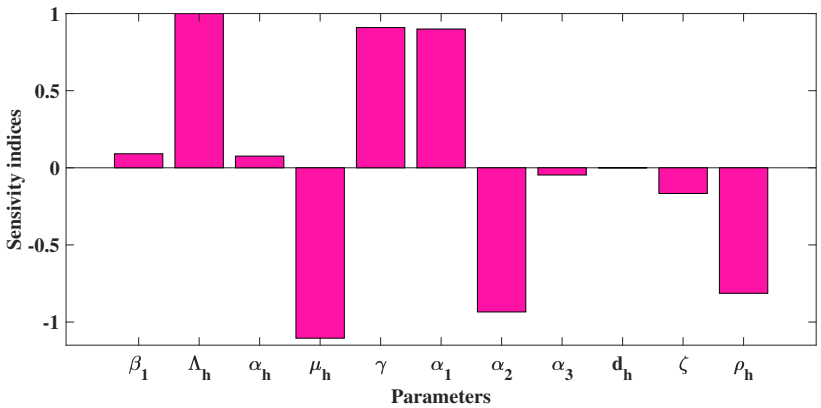

Figure 2: Sensitivity of R_0 with respect to the human parameters defining it.

Now $\mathbb{F}$ and $\mathbb{V}$ can be represented as

$$\mathbb{F} = \begin{bmatrix} 0 & 0 & \beta_1 S_h^0 + \gamma V_h^0 & 0 & 0 & \beta_2 S_h^0 \\ 0 & 0 & 0 & 0 & 0 & 0 \\ 0 & 0 & 0 & 0 & 0 & 0 \\ 0 & 0 & 0 & 0 & 0 & 0 \\ 0 & 0 & 0 & 0 & 0 & \delta_r S_r^0 \\ 0 & 0 & 0 & 0 & 0 & 0 \end{bmatrix},$$

$$\mathbb{V} = \begin{bmatrix} \kappa_1 & 0 & 0 & 0 & 0 & 0 \\ -\alpha_2 & \kappa_2 & 0 & 0 & 0 & 0 \\ -\alpha_1 & 0 & \kappa_3 & 0 & 0 & 0 \\ \alpha_3 & -\tau_2 & -\zeta & \kappa_4 & 0 & 0 \\ 0 & 0 & 0 & 0 & \kappa_5 & 0 \\ 0 & 0 & 0 & 0 & -\alpha_4 & \kappa_6 \end{bmatrix}.$$

Where

$$\begin{aligned} \kappa_1 &= (\mu_h + \alpha_1 + \alpha_2 + \alpha_3), \\ \kappa_2 &= (\zeta + \mu_h + d_h + \tau_1 + \tau_2), \\ \kappa_3 &= (\mu_h + d_h + \zeta + \rho_h), \\ \kappa_4 &= (\beta + \mu_h + d_h), \\ \kappa_5 &= (\mu_r + \alpha_4), \\ \kappa_6 &= (\mu_r + d_r + \rho_r). \end{aligned}$$

The fundamental reproduction number is denoted by R_0, and according to Dikemann [19], R_0 is regarded as the spectral region of the next-generation matrix. Upon analyzing the aforementioned matrix, we obtain the two largest eigenvalues, which are as follows:

$$R_{0,h} = \frac{(\beta_1 S_h^0 + \gamma V_h^0)\alpha_1}{(\alpha_1 + \alpha_2 + \alpha_3 + \mu_h)(d_h + \mu_h + \zeta + \rho_h)}, \qquad R_{0,r} = \frac{\delta_r S_r^0 \alpha_4}{(\alpha_4 + \mu_r)(d_r + \mu_r + \rho_r)}$$

$R_0 = \{R_{0,h}, R_{0,r}\}$.

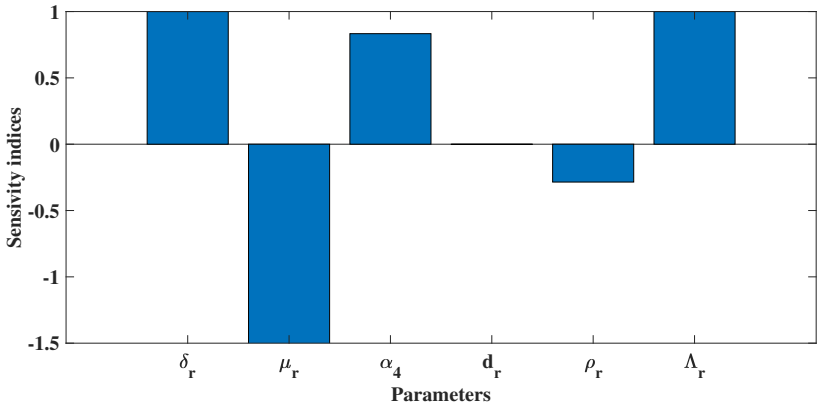

Figure 3: Sensitivity of R_0 with respect to the rodent parameters defining it.

5. Stability analysis of DFE

Theorem 5.1 *When $R_0 > 1$ for the DFE point $E^0\left(\frac{\Lambda_h}{\alpha_h+\mu_h}, \frac{\alpha_h\Lambda_h}{\mu_h(\alpha_h+\mu_h)}, 0, 0, 0, 0, 0, \frac{\Lambda_r}{\mu_r}, 0, 0, 0\right)$ are exists and it is locally asymptotically stable, otherwise it is unstable.*

Proof 5.1 *The Jacobian matrix of the system is calculated to assess the local stability of $E^0\left(\frac{\Lambda_h}{\alpha_h+\mu_h}, \frac{\alpha_h\Lambda_h}{\mu_h(\alpha_h+\mu_h)}, 0, 0, 0, 0, 0, \frac{\Lambda_r}{\mu_r}, 0, 0, 0\right)$ for the DFE is given by*

$$J_{E^0} = \begin{bmatrix} -A & 0 & 0 & \xi & \frac{-\beta_1\Lambda_h}{\alpha_h+\mu_h} & 0 & 0 & 0 & 0 & \frac{-\beta_2\Lambda_h}{\alpha_h+\mu_h} & 0 \\ \alpha_h & -\mu_h & 0 & 0 & \frac{-\gamma\alpha_h\Lambda_h}{\mu_h(\alpha_h+\mu_h)} & 0 & 0 & 0 & 0 & 0 & 0 \\ 0 & 0 & -B & 0 & \frac{\beta_1\Lambda_h}{\alpha_h+\mu_h} + \frac{\gamma\alpha_h\Lambda_h}{\mu_h(\alpha_h+\mu_h)} & 0 & 0 & 0 & 0 & \frac{\beta_2\Lambda_h}{\alpha_h+\mu_h} & 0 \\ 0 & 0 & \alpha_2 & -C & 0 & 0 & 0 & 0 & 0 & 0 & 0 \\ 0 & 0 & \alpha_1 & 0 & -D & 0 & 0 & 0 & 0 & 0 & 0 \\ 0 & 0 & \alpha_3 & \tau_2 & \zeta & -E & 0 & 0 & 0 & 0 & 0 \\ 0 & 0 & 0 & \tau_1 & \rho_h & \beta & -\mu_h & 0 & 0 & 0 & 0 \\ 0 & 0 & 0 & 0 & 0 & 0 & 0 & -\mu_r & 0 & \frac{-\delta_r\Lambda_r}{\mu_r} & 0 \\ 0 & 0 & 0 & 0 & 0 & 0 & 0 & 0 & -F & \frac{\delta_r\Lambda_r}{\mu_r} & 0 \\ 0 & 0 & 0 & 0 & 0 & 0 & 0 & 0 & \alpha_4 & -G & 0 \\ 0 & 0 & 0 & 0 & 0 & 0 & 0 & 0 & 0 & \rho_r & -\mu_r \end{bmatrix}.$$

Where,

$$\begin{aligned} &\mu_h + \alpha_h = A, \\ &\mu_h + \alpha_1 + \alpha_2 + \alpha_3 = B, \\ &\tau_1 + \tau_2 + \alpha_h + d_h + \mu_h + \xi = C, \\ &\zeta + d_h + \mu_h + \rho_h = D, \\ &\mu_h + \beta + d_h = E, \\ &\mu_r + \alpha_4 = F, \\ &d_r + \mu_r + \rho_r = G. \end{aligned}$$

Based on the matrix presented, we can readily identify seven eigenvalues as outlined below: $\lambda_1 = -\mu_r$, $\lambda_2 = -\mu_r$, $\lambda_3 = -\mu_h$, $\lambda_4 = -\mu_h$, $\lambda_5 = -(\mu_h + \beta + d_h)$ $\lambda_6 = -\mu_h - \alpha_h$, $\lambda_7 = -(\tau_1 + \tau_2 + \alpha_h + d_h + \mu_h + \xi)$.

The provided equations can be utilized to determine the remaining eigenvalues λ_i (for $i = 8, 9, 10, 11$),

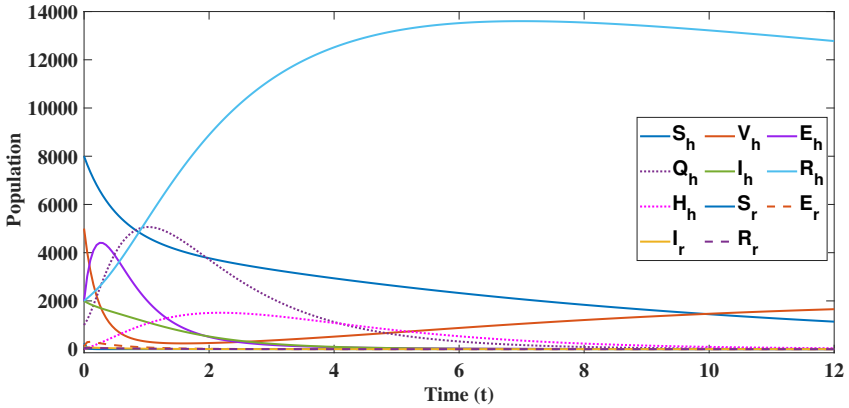

Figure 4: Dynamical behaviour of both population on time.

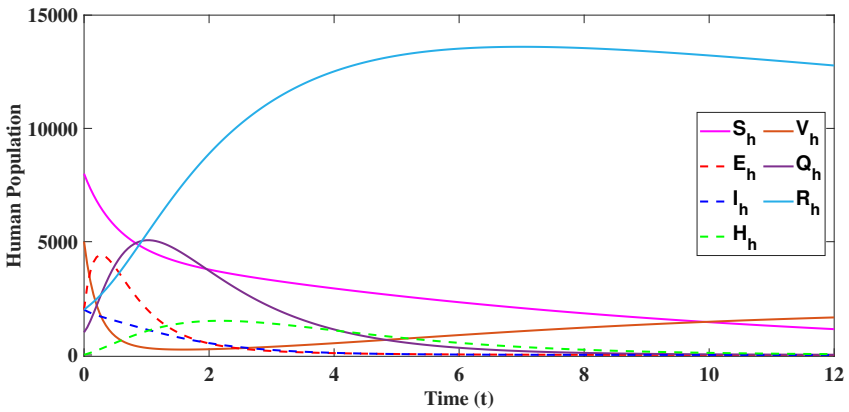

Figure 5: Dynamical behaviour of human population on time.

$$\lambda^2 + (B+D)\lambda + BD - \alpha_1\Big(\frac{\beta_1\Lambda_h}{\alpha_h+\mu_h} + \frac{\gamma\alpha_h\Lambda_h}{\mu_h(\alpha_h+\mu_h)}\Big) = 0, \tag{5.1}$$

$$\lambda^2 + (F+G)\lambda + FG - \alpha_4\frac{\delta_r\Lambda_r}{\mu_r} = 0. \tag{5.2}$$

As $B+D>0$, $BD-\alpha_1\Big(\frac{\beta_1\Lambda_h}{\alpha_h+\mu_h}+\frac{\gamma\alpha_h\Lambda_h}{\mu_h(\alpha_h+\mu_h)}\Big)>0$, *utilizing the Routh-Hurwitz criteria, Equation (5.1) possesses the pair of roots with a negative real part. Furthermore, since* $F+G>0, FG-\alpha_4\frac{\delta_r\Lambda_r}{\mu_r}>0$ *when* $R_0^h<1$, *applying the Routh–Hurwitz criterion, It can be concluded that Equation (5.2) possesses two roots with negative real parts as well.*

All eigenvalues derived from the Jacobian matrix J_{E^0} *demonstrate a characteristic where their non-negative elements are negative where* R_0 *is less than 1, a condition satisfied by both* R_0^h *and* R_0^r. *This brings us to the theorem.*

6. Sensitivity analysis

We analyse the effects of the parameter values, which should be categorized for dominating the infectious diseases, It may be accomplished via ascertaining the toughness of coordinate among every parameter in the model to control the fundamental reproduction number R_0 by using the partial order

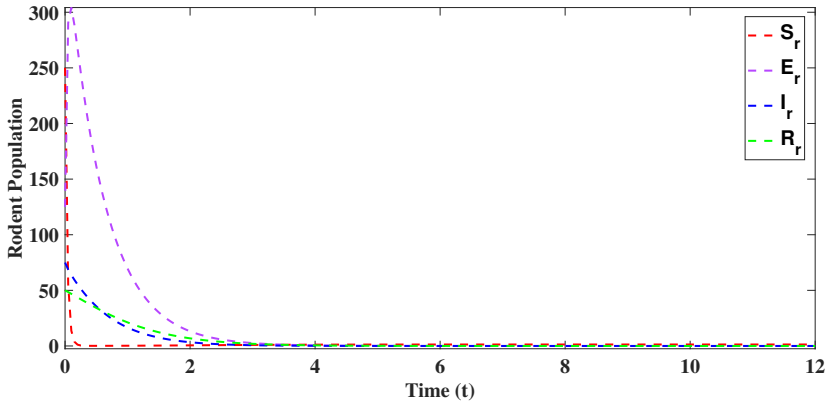

Figure 6: Dynamical behaviour of rodent population on time.

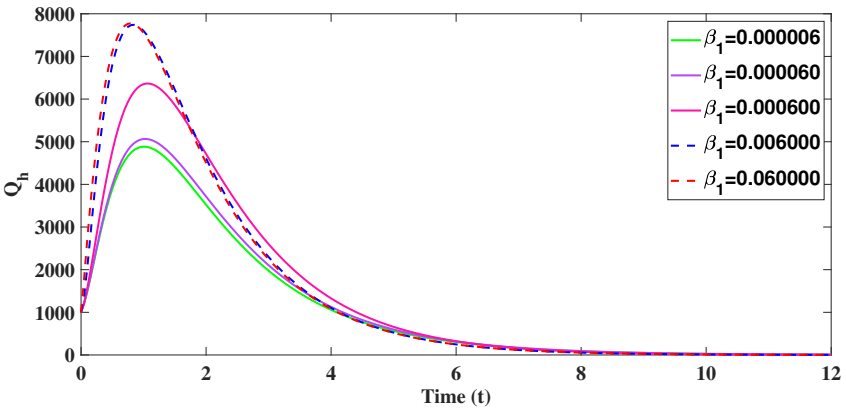

Figure 7: Variation of human quarantined population on time at the rate of β_1.

correlation coefficient [23,24]. Now we tested a significant parameters of R_0. The findings of the sensitivity analysis are shown in Figures 2 and 3. Now we obtain the sensitivity analysis of R_0 for each parameters by using analytical expression given as

$S_p^{R_0} = \frac{p}{R_0} \times \frac{\partial R_0}{\partial p}$,

Where p is any parameter contained in R_0. With the regarding of the above formulae, we analyse sensitivity indices and results are shown in Figures 2 and 3.

7. Numerical simulation and discussion

For the vital result of this $S_hV_hE_hQ_hI_hH_hR_hS_rE_rI_rR_r$ model (2.1) of the MPXV, we also use ODE45 test in MATLAB and evaluate the variables that are best fit in our $S_hV_hE_hQ_hI_hH_h\ R_hS_rE_rI_rR_r$ model. The suggested $S_hV_hE_hQ_hI_hH_hR_hS_rE_rI_rR_r$ model system (2.1) has 23 parameters listed above with their references and values. We describe results of the model (2.1) graphically by applying some estimated and discussed parameters from Table 1.

Figure 4 illustrates the temporal dynamics of the total population (human and rodent) over several months. The susceptible human population steadily decreases while the recovered human population correspondingly increases, indicating successful disease progression towards recovery. Figure 5 further highlights the positive impact of vaccination, where an increase in recovered humans corresponds with vaccine rollout. In contrast, Figure 6 shows a general decline in the rodent population compartments over time, reflecting the effect of disease and control measures on the vector population.

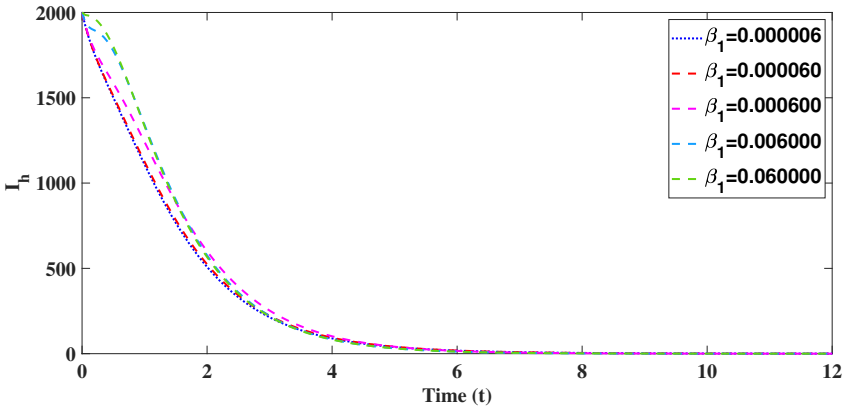

Figure 8: Variation of infected human population on time at the rate of β_1.

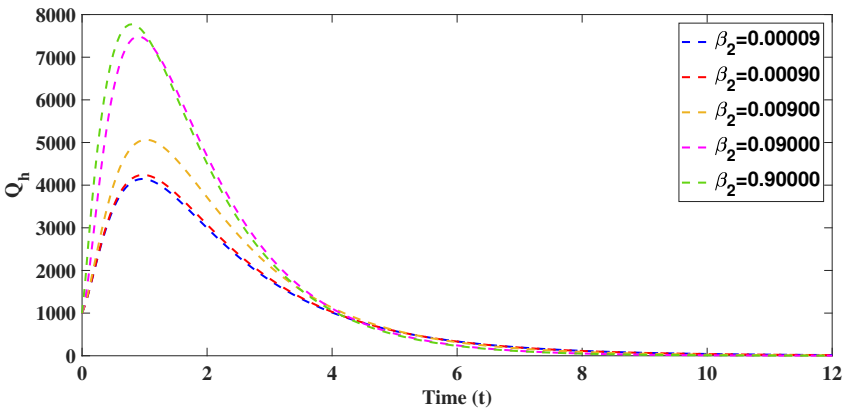

Figure 9: Variation of human quarantined population on time at the rate of β_2.

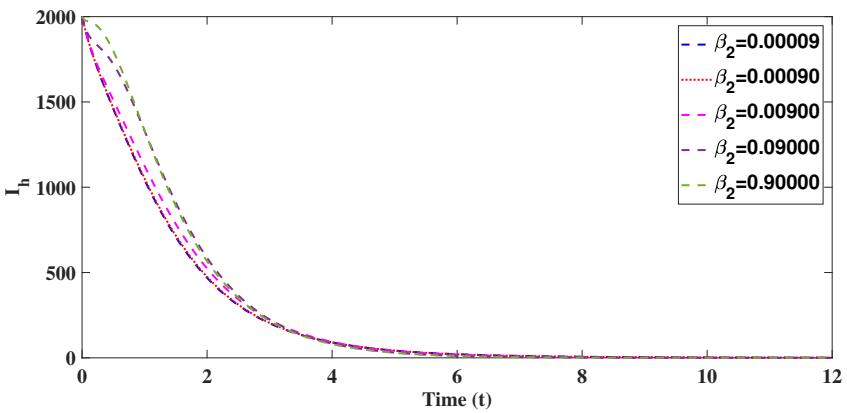

Figure 10: Dynamical behaviour of human infected population on time at the rate of β_2.

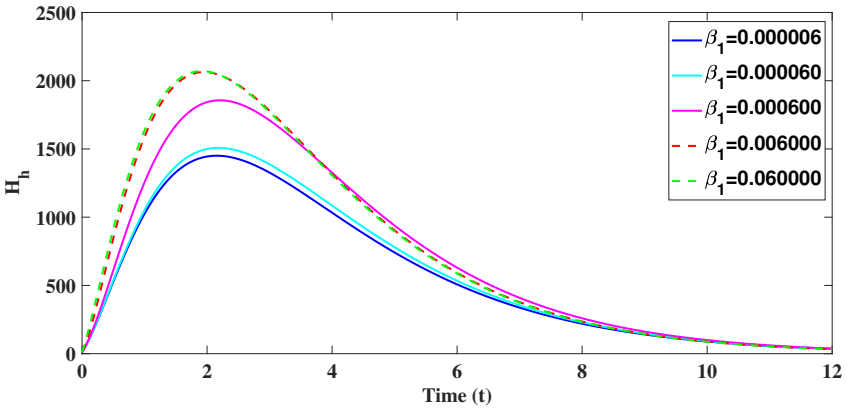

Figure 11: Dynamical behaviour of human hospitalised population on time at the rate of β_1.

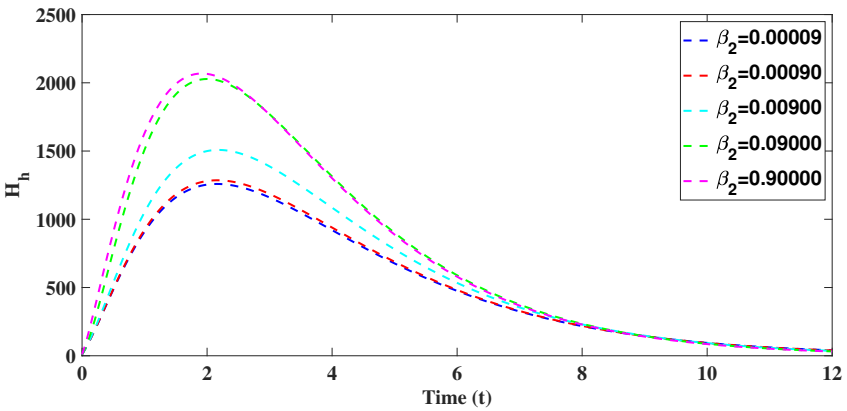

Figure 12: Dynamical behaviour of human hospitalised population on time at the rate of β_2.

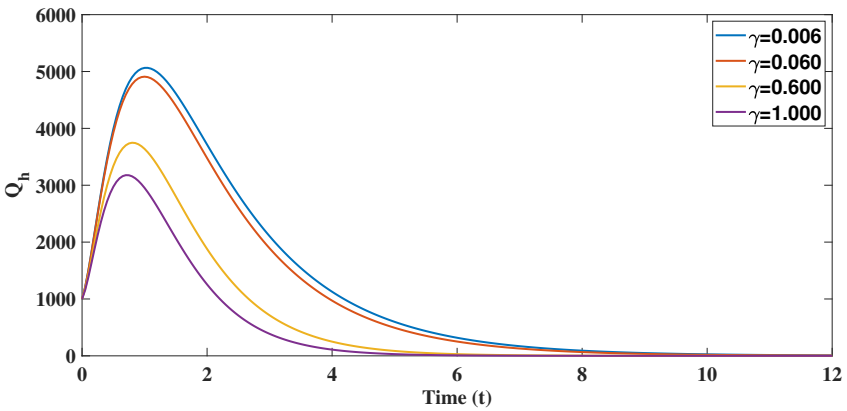

Figure 13: Dynamical behaviour of quarantined human population on time at the rate of γ.

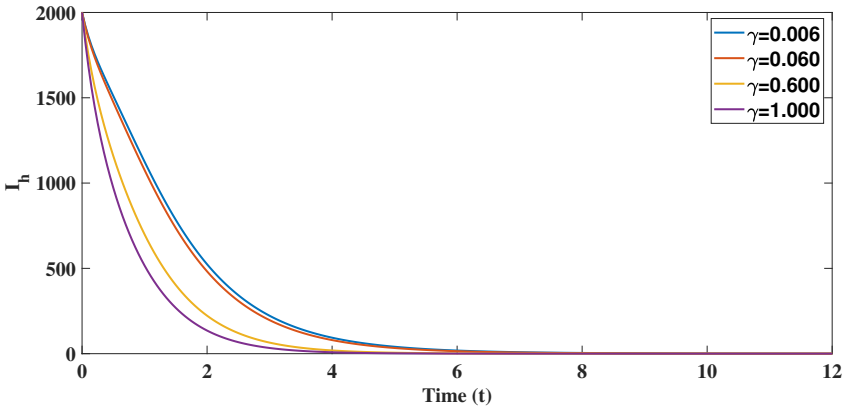

Figure 14: Dynamical behaviour of infected human population on time at the rate of γ.

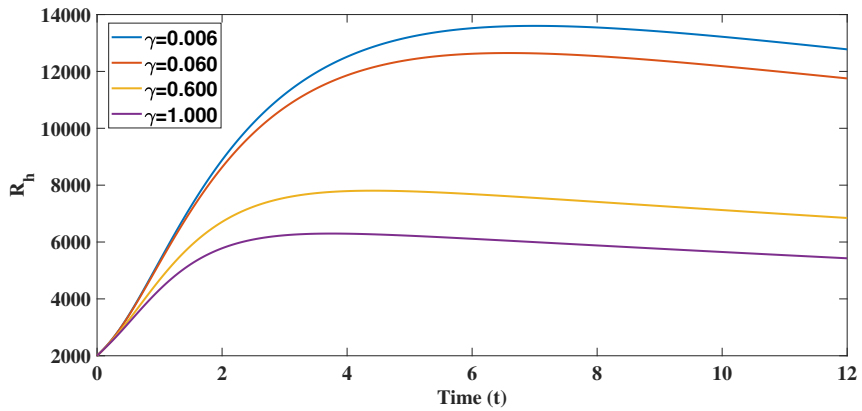

Figure 15: Dynamical behaviour of recovered human population on time at the rate of γ.

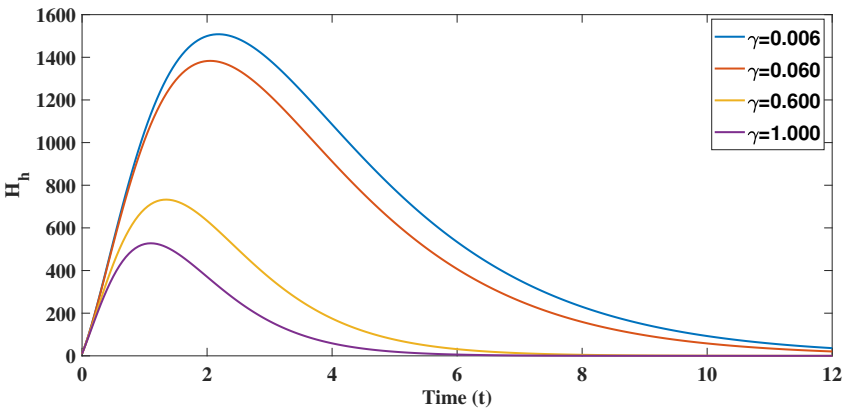

Figure 16: Dynamical behaviour of hospitalised human population on time at the rate of γ.

Parameter	Value	References	Parameter	Value	References
Λ_h	0.029	[20]	μ_h	0.02	[20]
α_h	0.1	[21]	ρ_r	0.6	[20]
ξ	0.2	[22]	γ	0.006	Assumed
α_1	0.2	[17]	α_2	2	[17]
α_3	0.1	Assumed	α_4	0.3	[21]
d_h	0.0002	Estimated [17]	ρ_h	0.83	[20]
ζ	0.17	Assumed	τ_1	0.52	[17]
τ_2	0.2	Assumed	β	0.5	Assumed
β_1	0.00006	[17, 20]	β_2	0.009	[17, 20]
Λ_r	2	[20]	μ_r	1.5	[20]
δ_r	0.4	[20]	d_r	0.0023	Assumed

Table 1: Description of parameters in the model.

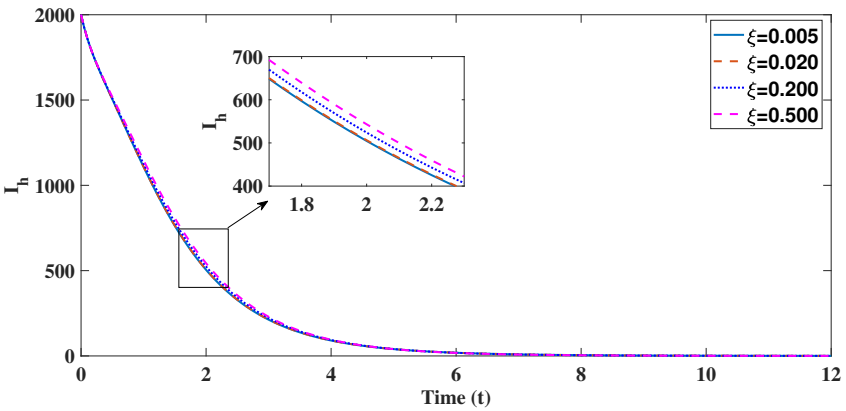

Figure 17: Dynamical behaviour of infected human population on time at the rate of ξ.

Figures 7 and 8 explore the influence of the parameter β_1 on quarantined and infected humans. As β_1 increases, more individuals enter quarantine, leading to a reduction in active infections, which underscores the effectiveness of quarantine as a control strategy. Similarly, Figures 9 and 10 demonstrate that increasing β_2 also raises quarantine numbers while decreasing infections, reinforcing the importance of timely isolation measures. Hospitalized population dynamics depicted in Figures 11 and 12 show an increasing trend with rising β_1 and β_2, highlighting the critical role of healthcare capacity in managing disease burden.

The parameters' effects on quarantined, infectious, recovered, and hospitalized populations are further analyzed in Figures 13 to 16 at varying rates γ. These results reveal that quarantined and hospitalized populations initially rise and then decline over time, while infectious cases steadily decrease and recovered cases increase, suggesting effective control interventions. Figure 17 illustrates the decrease in infected human population with an increase in the recovery rate ξ, emphasizing the importance of improving treatment and recovery processes.

The model has been simulated using the initial conditions: $S_h(0) = 8000$, $V_h(0) = 5000$, $E_h(0) = 2000$, $Q_h(0) = 1000$, $I_h(0) = 2000$, $R_h(0) = 2000$, $S_r(0) = 250$, $E_r(0) = 125$, $I_r(0) = 75$, $R_r(0) = 50$, $H_h(0) = 10$.The simulation results indicate that integrating vaccination, quarantine, and hospitalization strategies can effectively reduce the spread of monkeypox. These findings highlight the importance of achieving high vaccination coverage, prompt isolation of infected individuals, and sufficient hospital resources to control outbreaks. Additionally, managing the rodent vector population plays a critical role in preventing zoonotic transmission.

8. Conclusion and future scope

This study presents a comprehensive compartmental model for the transmission dynamics of monkeypox virus (MPXV) in human and rodent populations. Our analysis shows that maintaining high vaccination coverage and robust quarantine and hospitalization protocols effectively reduce disease spread and help contain potential epidemics, as indicated by the basic reproduction number (R_0). If $R_0 > 1$, MPXV has epidemic potential, whereas $R_0 < 1$ suggests eventual disease elimination or endemic stability. From a policy perspective, our findings advocate for integrated public health interventions combining vaccination campaigns, early case detection with quarantine, and strengthening healthcare infrastructure to manage hospitalizations. Additionally, vector control through rodent population management should be prioritized to minimize zoonotic spillover risks.

Future work may extend this model by incorporating age-structured populations and delay differential equations to capture latency and incubation periods better, as demonstrated in [25]. Furthermore, control strategies like awareness programs can enhance understanding of their role in transmission reduction [26]. Incorporating fractional-order derivatives may also provide deeper insight into memory effects in disease progression, potentially improving predictive accuracy and intervention planning [9, 27].

Declaration of competing interest: The authors declare that they have no known competing financial interests or personal relationships that could have appeared to influence the work reported in this paper.
Funding: This study received no specific financial support.
Data availability: No data was used for the research described in the article.

References

1. PV Magnus, EK Andersen, KB Petersen, and AB Andersen. A pox-like disease in cynomolgus monkeys. 1959.
2. Z Jezek, M Szczeniowski, KM Paluku, M Mutombo, and B Grab. Human monkeypox: confusion with chickenpox. *Acta tropica*, 45(4):297–307, 1988.
3. KN Durski. Emergence of monkeypox—west and central africa, 1970–2017. *MMWR. Morbidity and mortality weekly report*, 67, 2018.
4. M Manivel, A Venkatesh, and S Kumawat. Numerical simulation for the co-infection of monkeypox and HIV model using fractal-fractional operator. *Modeling Earth Systems and Environment*, 11(3):157, 2025.
5. JP Thornhill, S Barkati, S Walmsley, J Rockstroh, A Antinori, LB Harrison, R Palich, A Nori, I Reeves, MS Habibi, et al. Monkeypox virus infection in humans across 16 countries—april–june 2022. *New England Journal of Medicine*, 387(8):679–691, 2022.
6. GD Huhn, AM Bauer, K Yorita, MB Graham, J Sejvar, A Likos, IK Damon, MG Reynolds, and MJ Kuehnert. Clinical characteristics of human monkeypox, and risk factors for severe disease. *Clinical infectious diseases*, 41(12):1742–1751, 2005.
7. H Adler, S Gould, P Hine, LB Snell, W Wong, CF Houlihan, JC Osborne, T Rampling, MBJ Beadsworth, CJA Duncan, et al. Clinical features and management of human monkeypox: a retrospective observational study in the UK. *The Lancet Infectious Diseases*, 22(8):1153–1162, 2022.
8. ID Ladnyj, P Ziegler, and E Kima. A human infection caused by monkeypox virus in basankusu territory, democratic republic of the congo. *Bulletin of the World Health Organization*, 46(5):593, 1972.
9. K Soni and AK Sinha. Modeling marburg virus control with limited hospital beds: a fractional approach. *Physica Scripta*, 100(1):015251, 2024.
10. M Manivel, A Venkatesh, KA Kumar, MP Raj, SE Fadugba, and M Kekana. Quantitative modeling of monkeypox viral transmission using caputo fractional variational iteration method. *Partial Differential Equations in Applied Mathematics*, 13:101026, 2025.
11. R Kaur, Prabhanshi Jhamb, and P Verma. Transmission dynamics of COVID-19 across a region: A mathematical model. *Proceedings of the National Academy of Sciences, India Section A: Physical Sciences*, 1–16, 2025.
12. BE Cunha. Monkeypox in the united states: an occupational health look at the first cases. *AAOHN Journal*, 52(4): 164–168, 2004.
13. KD Reed, JW Melski, MB Graham, RL Regnery, MJ Sotir, MV Wegner, JJ Kazmierczak, EJ Stratman, Y Li, JA Fairley, et al. The detection of monkeypox in humans in the western hemisphere. *New England Journal of Medicine*, 350(4):342–350, 2004.
14. Shyamsunder and M Meena. A comparative analysis of vector-borne disease: monkeypox transmission outbreak. *Journal of Applied Mathematics and Computing*, pages 1–37, 2025.
15. E Alakunle, U Moens, G Nchinda, and MI Okeke. Monkeypox virus in nigeria: infection biology, epidemiology, and evolution. *Viruses*, 12(11):1257, 2020.

16. M Manivel, A Venkatesh, and S Kumawat. A comprehensive study of monkeypox disease through fractional mathematical modeling. *Mathematical Modelling and Numerical Simulation with Applications*, 5(1):65–96, 2025.

17. OJ Peter, S Kumar, N Kumari, FA Oguntolu, K Oshinubi, and R Musa. Transmission dynamics of monkeypox virus: a mathematical modelling approach. *Modeling Earth Systems and Environment*, pages 1–12, 2022.

18. PVD Driessche and J Watmough. Further notes on the basic reproduction number. *Mathematical epidemiology*, pages 159–178, 2008.

19. O Diekmann, JAP Heesterbeek, and MG Roberts. The construction of next-generation matrices for compartmental epidemic models. *Journal of the royal society interface*, 7(47):873–885, 2010.

20. CP Bhunu and S Mushayabasa. Modelling the transmission dynamics of pox-like infections. *IAENG International Journal of Applied Mathematics*, 2(41), 2011.

21. S Usman and II Adamu. Modeling the transmission dynamics of the monkeypox virus infection with treatment and vaccination interventions. *Journal of Applied Mathematics and Physics*, 5(12):2335, 2017.

22. JP Singh, S Kumar, D Baleanu, and KS Nisar. Monkeypox viral transmission dynamics and fractional-order modeling with vaccination intervention. *Fractals*, 31(10):2340096, 2023.

23. LK Yan. Application of correlation coefficient and biased correlation coefficient in related analysis. *Journal of Yunnan university of Finance and Economics*, 19(3):78–80, 2003.

24. S Marino, IB Hogue, CJ Ray, and DE Kirschner. A methodology for performing global uncertainty and sensitivity analysis in systems biology. *Journal of theoretical biology*, 254(1):178–196, 2008.

25. MP Raj, A Venkatesh, KA Kumar, and M Manivel. Dengue transmission model in an age-structured population using delay differential equations. *Discover Public Health*, 22(1):1–20, 2025.

26. FM Mrope, OJ Kigodi, N Jeeva, and M Manivel. Mathematical modeling of the impact of insecticides on the transmission dynamics of maize streak disease. *Modeling Earth Systems and Environment*, 11(4):264, 2025.

27. K Soni and AK Sinha. Dynamics of epidemic model with conformable fractional derivative. *Nonlinear Science*, page 100040, 2025.

[1] *Department of Mathematics, Agra College, Agra, Dr. Bhim Rao Ambedkar University, Agra, India*
E-mail address: himanigarg23.hg@gmail.com, atarsingh1968@gmail.com

and

[2] *Department of Mathematics, SRM University Delhi-NCR, Sonepat-131029, Haryana, India*
E-mail address: skumawatmath@gmail.com

and

[3] *Department of HEAS (Mathematics), Rajasthan Technical University, Kota, India*
E-mail address: sunil_a_purohit@yahoo.com

and

[4] *Department of Electronics and Communication Engineering, Saveetha School of Engineering, SIMATS, Chennai, Tamilnadu, India*

and

[5] *Siirt University, Art and Science Faculty, Department of Mathematics, 56100 Siirt, Turkey*

and

[6] *Department of Computer Engineering, Biruni University, 34010 Topkapı, Istanbul, Turkey*

and

[7] *Near East University, Mathematics Research Center, Department of Mathematics, Near East Boulevard, PC: 99138, Nicosia /Mersin 10 – Turkey*

and

[8] *Applied Science Research Center, Applied Science Private University, Amman, Jordan*
E-mail address: aliakgul00727@gmail.com